TECHNISCHE MECHANIK
an open access journal

journal homepage: www.ovgu.de/techmech

Tech. Mech., Vol. 42, Is. 1, (2022), 36–52

Received: 15.06.2022
Accepted: 30.11.2022
Available online: 12.12.2022

Vibration Analysis of Nonlinear Magneto Flexoelectric Mass Sensor Carbon Nanotube Resting on Elastic Substrate

R. Selvamani[1]*, M. Mahaveer Sree Jayan[2], J. Nicholas George[3] and Farzad Ebrahimi[4]

[1] Department of Mathematics, Karunya Institute of Technology and Sciences, Coimbatore - 641 114, Tamilnadu, India
[2] Department of Mathematics, Indra Ganesan College of Engineering, Tiruchirappalli - 620 012, Tamilnadu, India
[3] Department of Mathematics, Indira Gandhi College of Special Education, Coimbatore - 641 108, Tamilnadu, India
[4] Department of Mechanical Engineering, University of Tehran, North Karegar Ave. Tehran, Iran

Abstract: The present paper is dedicated to study the nonlinear ultrasonic waves in a magneto-flexo-thermo elastic armchair single-walled carbon nanotube with mass sensors resting on polymer matrix. Here the small-scale effect is captured by Eringen's nonlocal elasticity theory. After developing the formal solution of the mathematical model consisting of partial differential equations, the frequency equations have been analyzed numerically by using the nonlinear foundations supported by Winkler-Pasternak model. The solution is obtained by ultrasonic wave dispersion relations. Parametric work is carried out to scrutinize the influence of the nonlocal scaling, magneto-flexoelectric mechanical loadings, foundation parameters, attached mass, various boundary condition and length on the dimensionless frequency of nanotube. It is noticed that the boundary conditions, nonlocal parameter, attached mass and tube geometrical parameters have significant effects on dimensionless frequency of nanotubes.

Keywords: Nonlocal elasticity; Flexoelectric; Armchair; Mass sensor; CNT; Euler-beam theory; NEMS.

1 Introduction

The advancement of nano structures has been enhanced through the coupling of magneto-flexo-thermo-elasticity in armchair single-walled carbon nanotube(SWCNT). Using MFT based nano materials in polymer matrix as surrounding medium to generate better efficiency of embedded nano structures has been attracting great research attention in recent years (Ebrahimi and Dabbagh (2018)). Due to the arrival of nonlocal continuum theory, the nonlocal Euler-Bernoulli and Timoshenko beam models enable the assessment of scaling effect on a carbon nanotube's(CNT's) dispersion relations. Wang (2005), H. Heireche (2008), Eringen (2002), A. C. Eringen (1972) and Eringen (1983) elaborated the nonlocal continuum field theories and validated in different nano materials. L. Wang (2006) carried out the nonlocal continuum models to investigate the small scale effect on elastic buckling of CNTs and referred the impact of small scale effect on vibration modes. B. Fang (2013) has discussed the nonlinear free vibration of double walled CNTs based on the nonlocal elasticity theory. They found that the surrounding elastic medium plays an important role in the nonlinear propagation and the amplitude development. Z. Saadatnia (2017) investigated the nonlinear harmonic vibration of a piezoelectric-layered nanotube conveying fluid flow and concluded that the effects of small scale parameter is quite considerable in the frequency responses of the system in the presence of fluid environment. H. Askari (2017) presented the forced vibration of fluid conveying CNTs considering thermal effect and nonlinear foundations. B. Gheshlaghi (2011) read the forced vibration of fluid conveying CNTs considering thermal and nonlinear vibrational behaviour of homogenous nanobeams.

M. Sadeghi-Goughari (2017) studied the vibrational behaviour of a CNT conveying magnetic fluid subjected to a longitudinal magnetic field. Y. Zhen (2019) verified the free vibration of viscoelastic nanotube under longitudinal magnetic field and indicated the fact that the first natural frequency increases slightly with the increase of the nonlocal parameter, while higher natural frequencies decrease significantly with the increase of the nonlocal parameter. H. Dai (2018) explored the exact modes for post-buckling characteristics of nonlocal nanobeams in a longitudinal magnetic field. Ebrahimi and Barati (2017b) investigated the propagation of waves in nonlocal porous multi-phase nano crystalline nanobeams via longitudinal magnetic field effect. They pointed out the concept that the wave frequencies and phase velocities may increase or decrease with the reduction in the inhomogeneity magnitudes. L. Li (2016) illustrated the wave propagation in viscoelastic SWCNTs with surface effect under magnetic field based on nonlocal strain gradient theory and concluded with the importance of damping coefficient. A. G. Arani (2016) discussed the longitudinal magnetic field effect on wave propagation of fluid-conveyed SWCNT using Knudsen number and surface considerations. D. Zhang (2016) studied the vibration analysis of horn-shaped SWCNTs embedded in viscoelastic medium via a longitudinal magnetic field. A two scale coefficient model is developed to study the propagation of longitudinal stress waves under a longitudinal magnetic field by Güven (2015) via a unified nonlocal elasticity theory. Q. Wang (2006) validated the nonlocal elastic shell model for studying longitudinal waves in SWCNT and found that the microstructure and the coupling of the longitudinal wave and radial motion play a vital role in the dispersion of waves. Azarboni (2019) explored the magneto-thermal primary frequency response analysis of CNT considering surface effect under different boundary conditions. They inferred that the increase in longitudinal magnetic field leads to shifting the backward jumping at higher excitation amplitude values for different

* E-mail address: selvam1729@gmail.com
doi: 10.24352/UB.OVGU-2022-059

boundary conditions. S. Pradhan (2009) utilized the nonlocal continuum models to analyse the small scale effect on vibration of embedded multi-layered graphene sheets.

Thermal buckling properties of zigzag SWCNTs using a refined nonlocal model are investigated by A. Semmah (2014). They inferred that the thermal buckling properties of SWCNTs are strongly dependent on the scale effect and additionally on the chirality of zigzag CNT. M. Naceri (2011) presented the wave propagation in armchair SWCNTs under thermal environment. H. Baghdadi (2014) noted the thermal effect on vibration characteristics of armchair and zigzag SWCNTs using nonlocal parabolic beam theory. They indicated the significant dependence of natural frequencies on the temperature change as well as the chirality of armchair and zigzag CNT. The thermal effect on vibration of SWCNTs using nonlocal Timoshenko beam theory is investigated by A. Benzair (2008). It is concluded that the effects lead to a decrease in frequencies when compared with those obtained by the Euler beam model. A. Besseghier (2011) presented the thermal effect on wave propagation in double-walled CNTs embedded in a polymer matrix using nonlocal elasticity. Y. Q. Zhang (2007) studied the thermal effects on interfacial stress transfer characteristics of single/multi-walled carbon nano tubes/polymer composite systems under thermal loading by means of thermoelastic theory and conventional fiber pullout models. P. Lata (2019a) and P. Lata (2019b) despite several researchers, worked on different theory of thermoelasticity. P. Lata (2016) and R. Kumar (2017) studied the deformation in transversely isotropic material using thermoelasticity.

S. Narendar (2011) predicted the nonlocal scaling parameter for armchair and zigzag SWCNTs through molecular structural mechanics, nonlocal elasticity and wave propagation technique. W. A. Bedia (2015) contributed the study on the thermal buckling characteristics of armchair SWCNT embedded in an elastic medium. M. Zidour (2014) developed the buckling analysis of chiral SWCNTs by using the nonlocal Timoshenko beam theory. T. Bensattalah (2016) investigated the thermal and chirality effects on vibration of SWCNTs embedded in a polymeric matrix using nonlocal elasticity theories. J. C. Hsu (2008) presented the resonance frequency of chiral SWCNTs using Timoshenko beam theory. Aydogdu (2012) studied the axial vibration of SWCNT embedded in an elastic medium and concluded with the fact that the axial vibration frequencies of SWCNT embedded in an elastic medium highly over estimated by the classical rod model because of ignoring the effect of small length scale. R. Ansari (2012) pointed out the dynamic stability of embedded SWCNTs including thermal environment effects and inferred the result that the difference between instability regions predicted by local and nonlocal beam theories is significant for nanotubes with lower aspect ratios.

Nano-scale structures coupled with mass sensors have been studied by scientist in recent years. D. H. Wu (2006) analysed the resonance frequency of a SWCNT via a continuum mechanics-based finite element method(FEM). H. Lee (2009) modeled CNT nano-mass sensors with molecular structural mechanics method. Another similar study on the application of this theory to examine the frequency shift behavior of plate-type nano-mass sensor made of FG nano structures was presented by M. R. Barati (2017). For example, the potential of SWCNT as a mass sensor is investigated using continuum mechanics theory by R. Chowdhury (2009). M. Arda (2020) have referred the effect of stiffness and mass ratios; attach point of the detected elastic mass, nonlocal parameter to non-dimensional frequency of the nano-mass sensor. H. Liu (2020) investigated a unique nanoscale mass sensor manufactured from clever FG-MEE core included with graphene layers in its pinnacle and backside surfaces. H. Lee (2010) developed the frequency shift and sensitivity of carbon nanotube based sensor with an attached mass using nonlocal elasticity theory.

K. Wang (2018) proposed an array of flexoelectric layered nanobeams for vibration energy harvesting. F. Ebrahimi (2019) investigated the surface effect on scale-dependent vibration behaviour of flexoelectric sandwich nanobeams and they found that contribution of flexoelectricity on the natural frequencies. R. Basutkar (2019) stated the static analysis of flexoelectric nanobeams incorporating surface effects using element free Galerkin method. M. A. Nematollahi (2019) discussed and developed to predict the mass ratio and fluid velocity of a piezoelectric nanotube conveying fluid. M. Aydogdu (2011) found an advanced elastic rod version and carried out to investigate the small-scale impact at the axial vibrations of SWCNTs with attached mass. R. Selvamani (2020) and R. Selvamani (2018) studied the dynamics of coated piezoelectric rod and nonlocal strain gradient buckling behaviour of single-layer graphene sheets in the hygro-thermal environment resting on the elastic medium. To the best of the author's knowledge, there has been no record regarding the nonlinear ultrasonic waves in a magneto-flexo-thermo elastic armchair SWCNT with mass sensors resting on polymer matrix via Eringen's nonlocal elasticity theory. Therefore, there is a strong scientific need to understand the nonlinear ultrasonic vibration behaviour of the armchair SWCNT with mass sensor resting on elastic substrate in magneto-thermo elastic environment.

In this paper, we considered the nonlinear magneto-flexo-thermo-elastic waves in an armchair SWCNT resting on polymer matrix is studied via Euler beam theory by considering the elasticity of attached mass sensors. The analytical formulation is developed based on Eringen's nonlocal elasticity theory to account small scale effect. The solution is obtained by ultrasonic wave dispersion relations. Parametric studies are conducted to scrutinize the influence of the magneto-electro-mechanical loadings, attached mass, nonlocal parameter and aspect ratio on the deflection characteristics of nanotube. The influence of each parameter is highlighted through a group of diagrams and tables.

2 Mathematical Formulations

2.1 Eringen nonlocal theory of elasticity

This theory assumes that stress state at a reference point x in the body is regarded to be dependent not only on the strain state at x but also on the strain states at the all-other points X' of the body. The general form of the constitutive equations in the nonlocal form of elasticity contains an integral over the entire region of interest. The integral contains a nonlocal kernel function, which describes the relative influences of the strains at various locations on the stress at a given location. The constitutive equations of linear, homogeneous, isotropic, nonlocal elastic solid with zero body forces are given by Eringen (2002), Eringen (1983) and A. C. Eringen (1972) as follows

$$\sigma_{ij,i} + \rho(f_j - \ddot{u}_j) = 0 \tag{1}$$

$$\sigma_{ij}(X) = \int_{\nu} \pi(|X - X'|, \tau)\sigma^c_{ij}(X')d\nu(X') \tag{2}$$

$$\sigma^c_{ij}(X') = C_{ijkl}\varepsilon_{ij}(X') \tag{3}$$

$$\varepsilon_{ij}(X') = \frac{1}{2}(u_{i,j} + u_{j,i}) \tag{4}$$

Eq.(1) is the equilibrium equation, where $\sigma_{ij,i}$, ρ, f_j, $\ddot{u}_j$ are the stress tensor, mass density, body force density and displacement vector at a reference point x in the body, respectively at the time t. Equation (3) is the classical constitutive relation where $\sigma^c_{ij}(X')$ is the classical stress tensor at any point X' in the body, which is related to the linear strain tensor $\varepsilon_{ij}(X')$ at the same point. Eq.(4) is the classical strain displacement relationship. The kernel function $\pi(|X - X'|, \tau)$ is the attenuation function which incorporated the nonlocal effect in the constitutive equations. The volume integral in Eq.(2) is over the region ν occupied by the body. It is clear that, the only difference between Eqs.(1)-(4) and the corresponding equations of classical elasticity in Eq.(2) replaces the Hooke's law in Eq.(3) by Eq.(2). Eq.(2) consists the parameters which correspond to the nonlocal modulus has dimensions of $(\text{length})^{-3}$ and so it depends on a characteristic length (lattice parameter, size of grain, granular distance, etc.). Therefore the nonlocal modulus can be written in the following form:

$$\pi = \pi(|X - X'|, \tau), \quad \tau = \frac{e_0 a}{l} \tag{5}$$

where e_0 is a constant corresponding to the material and has to be determined for each material independently. Here a and l are internal and external characteristic length of the system (wavelength, crack length, size or dimensions of sample, etc.). Then, the integro-partial differential Eq.(2) of nonlocal elasticity can be simplified to partial differential equation as follows

$$(1 - \tau^2 l^2 \nabla^2)\sigma_{ij}(X) = \sigma^c_{ij}(X) = C_{ijkl}\varepsilon_{ij}(X) \tag{6}$$

where ∇ denotes the second-order spatial gradient applied on the stress tensor σ_{ij} and $\tau = e_0 a/l$, C_{ijkl} is the elastic modulus tensor of classical isotropic elasticity and ε_{ij} is the strain tensor. Eringen proposed $e_0 = 0.39$ by the matching of the dispersion curves via nonlocal theory for place wave and born-Karman model of lattice dynamics at the end of the Brillouin zone ($ka = \pi$) where a is the distance between atoms and k is the wave number in the phonon analysis. A. C. Eringen (1972) proposed $e_0 = 0.31$ in his study for Rayleigh surface wave via nonlocal continuum mechanics and lattice dynamics.

2.2 Atomic structure of carbon nanotube

CNTs are considered to be tubes formed by rolling a graphene sheet about the $\overrightarrow{T}$. A vector perpendicular to $\overrightarrow{T}$ is the chiral vector denoted by $\overrightarrow{C_h}$. The chiral vector and corresponding chiral angle define the type of CNT, i.e., zigzag, armchair and chiral. $\overrightarrow{C_h}$ can be expressed with respect to two base vectors $\overrightarrow{a_1}$ and $\overrightarrow{a_2}$ as under

$$\overrightarrow{C_h} = n\overrightarrow{a_1} + m\overrightarrow{a_2} \tag{7}$$

where n and m are the indices of translation which decide the structure around the circumference. Figure 1 descripts the lattice of transition (n, m) along with the base vectors $\overrightarrow{a_1}$ and $\overrightarrow{a_2}$. If the indices of translation are such that $m = 0$ and $m = n$ then the corresponding CNT are categorized as zigzag and armchair respectively. Considering the chirality diameter and the chiral angle of the CNT, the chiral vector for each nanostructure is calculated. The diameter of armchair SWCNT for $(n = m)$ is given by Yamabe (1995):

$$d = \frac{3na}{\pi}. \tag{8}$$

Based on the link between molecular mechanics and solid mechanics, Y. Wu (2006) developed an energy-equivalent model for studying the mechanical properties of SWCNT. Using the same method, the equivalent Young's modulus of armchair nanotube are expressed as

$$E_{SWCNT} = \frac{4\sqrt{3KC}}{9Ct + 4Ka^2t(\gamma_{21}^2 + \gamma_{22}^2)} \tag{9}$$

where K and C are the force constants. t is thickness of the SWCNT and the parameters γ_{21} and γ_{22} are given by:

$$\gamma_{21} = \frac{-3\sqrt{4} - 3\cos^2(\pi/2n)\cos(\pi/2n)}{8\sqrt{3} - 2\sqrt{3}\cos^2(\pi/2n)} \tag{10}$$

$$\gamma_{22} = \frac{12 - 9\cos^2(\pi/2n)}{16\sqrt{3} - 4\sqrt{3}\cos^2(\pi/2n)}. \tag{11}$$

Letting $n \to \infty$ the expressions of Young's modulus of a graphite sheet is given by:

$$E_g = \frac{16\sqrt{3}Kt}{18Ct + Ka^2t}. \tag{12}$$

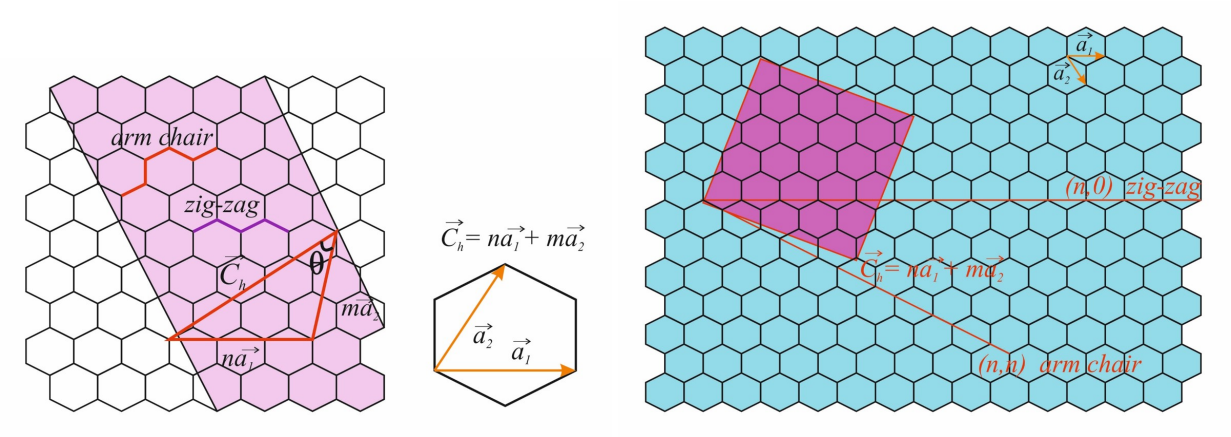

Fig. 1: (From left)(a) Geometric properties of SWCNT; (b) Graphene structure of carbon nanotube

2.3 Basic equations of magnetic field force

The CNTs appear in a hollow structure formed by covalently bonded carbon atoms, which can be imagined as a rectangular graphite sheet rolled from one side of its longest edge to form a cylindrical tube (shown in Fig. 2). A cylindrical coordinate system (X, θ, Z) is shown in Fig. 2. Here X expresses the longitudinal direction of shell, θ expresses the circumferential direction of uniform shell and Z expresses the radial direction, the surface defined by $Z = 0$ is set on the middle surface of the shell. Assuming that the magnetic permeability, η of CNTs equals the magnetic permeability of the medium around it, the Maxwell equations are given by

$$f = \nabla \times \overline{s}, \quad \nabla \times \tilde{e} = -\eta \frac{\partial \overline{s}}{\partial t}, \qquad div\, \overline{s} = 0, \tag{13}$$

$$\overline{s} = \nabla \times (\overline{U} \times \overline{H}), \quad \tilde{e} = -\eta \left(\frac{\partial \overline{s}}{\partial t} \times \overline{H} \right) \tag{14}$$

$f, \overline{s}, \tilde{e}$ and $\overline{U}$ represents the current density, strength vectors of electric field, displacement vectors of magnetic field and the vector of displacement respectively, ∇ is the Hamilton arithmetic operator of shell $\nabla = \left(\frac{\partial}{\partial X}\vec{i} + \frac{\partial}{\partial \theta}\vec{j} + \frac{\partial}{\partial R}\vec{k} \right)$. Applying a longitudinal magnetic field vector $\overline{H}(H_x, 0, 0)$ exerted on the i layer CNT with the cylindrical coordinate (X, θ, R) and the displacement vector $\overline{U} = (u_i, v_i, Y_i)$ of the i layer CNT to Eq.(13), yields

$$\overline{s} = \nabla \times (\overline{U} \times \overline{H}) = -\overline{H}_x \left(\frac{\partial v_i}{\partial \theta} + \frac{\partial Y_i}{\partial Z} \right) + \overline{H}_x \left(\frac{\partial v_j}{\partial X} \right) + \overline{H}_x \frac{\partial Y}{\partial X} k, \tag{15}$$

$$f = \nabla \times \overline{s} = \left(\overline{H}_x \left(-\frac{\partial^2 v_{\vec{i}}}{\partial X \partial R} + \frac{\partial^2 Y_{\vec{i}}}{\partial X \partial \theta} \right) - \overline{H}_x \left(\frac{\partial^2 v_{\vec{j}}}{\partial \theta \partial R} + \frac{\partial^2 Y_{\vec{j}}}{\partial X^2} + \frac{\partial^2 v_{\vec{j}}}{\partial R^2} \right) + \overline{H}_x \left(\frac{\partial^2 v_{\vec{k}}}{\partial X^2} + \frac{\partial^2 Y_{\vec{k}}}{\partial X^2} + \frac{\partial^2 v_{\vec{k}}}{\partial R^2} \right) \right). \tag{16}$$

The Lorentz force q induced by the longitudinal magnetic field can be written as

$$q(\overline{q_x}, \overline{q_\theta}, \overline{q_z}) = f \times B = f \times \eta \overline{H} = \eta \left(0\vec{i} + \overline{H}_x^2 \left(\frac{\partial^2 v_{\vec{j}}}{\partial X^2} + \frac{\partial^2 v_{\vec{j}}}{\partial \theta^2} + \frac{\partial^2 Y_{\vec{j}}}{\partial \theta \partial R} \right) + \overline{H}_x^2 \left(\frac{\partial^2 Y_{\vec{k}}}{\partial X^2} + \frac{\partial^2 Y_{\vec{k}}}{\partial \theta^2} + \frac{\partial^2 v_{\vec{k}}}{\partial \theta \partial R} \right) \right) \tag{17}$$

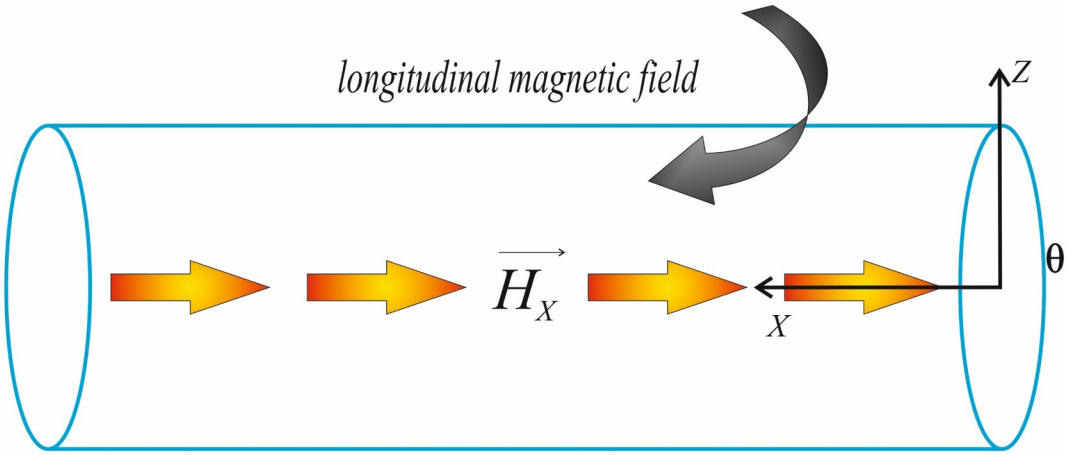

Fig. 2: Single-walled carbon nanotube subjected to axial magnetic field

where q_x, q_θ and q_z express the Lorentz force along the X, θ and R direction as follows (Fig.3):

$$\overline{q_x} = 0 \tag{18}$$

$$\overline{q_\theta} = \eta\left(\frac{H_x^2}{R^2}\frac{\partial^2 v_i}{\partial x^2} + H_x^2\frac{\partial^2 v_i}{\partial x^2}\right) \tag{19}$$

$$\overline{q_z} = \eta\left(H_x^2\frac{\partial^2 Y}{\partial X^2}\right) \tag{20}$$

The external force q_{mag} consists of the Lorentz force $\overline{q_z}$ due to the longitudinal magnetic field and the distributed transverse force F_s due to the effect of surface tension. Then we get,

$$q_{mag} = \overline{q_z}(x) + F_s \tag{21}$$

where the Lorentz force $\overline{q_z}$ is defined in Eq. (20) (L. Li (2016)) and the distributed transverse force F_s can be defined as(X. Lei (2012))

$$F_s = \left(H_s\frac{\partial^2 Y}{\partial X^2}\right) \tag{22}$$

Here η is the magnetic permeability, H_s is a constant, defined as

$$H_s = 2\mu(d+h) \tag{23}$$

where μ denotes the residual surface tension d is distance of CNT and h is the effective thickness of SWCNTs. The term $\overline{q_z}$ is the magnetic force per unit length due to Lorentz force exerted on the tube in Z-direction considered form when considering the effect of surface elasticity, the effect bending stiffness EI should be modified as (X. Lei (2012), Z. Yan (2011)).

$$EI^* = EI + Q_s E_s \tag{24}$$

where $Q_s = \frac{\pi}{8}(d+h)^3$. Here E_s denotes the surface Young's modulus, h is the effective thickness of SWCNTs and d is already denoted in Eq.(8).

3 Euler Bernoulli Beam Theory (EBT) based on Nonlocal Relations

The partial differential equation which governs the free vibration of nanotube under the influence of flexo-thermal and Lorentz force can be expressed as

$$\frac{\partial \Pi}{\partial X} + N_t\frac{\partial^2 Y}{\partial X^2} + q_{(mag)} + \beta y + f(x) = \rho A\frac{\partial^2 Y}{\partial t^2} \tag{25}$$

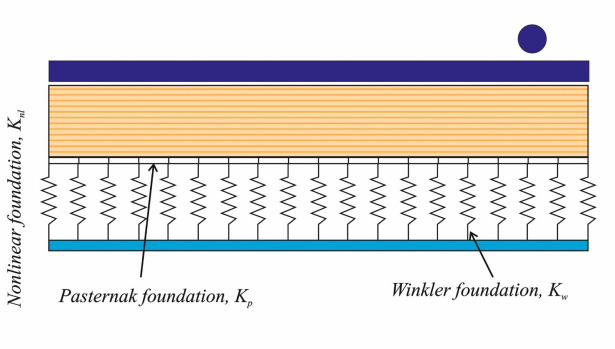

Fig. 3: From left (a) Geometry of SWCNT in flexoelectric with polymer matrix (b) Geometry of SWCNT in nonlinear foundation

where $f(x)$ is the interaction pressure per unit axial length between the nanotube and the surrounding elastic medium. A is the cross section of CNT.

$$\beta = \frac{f}{1 - \left(\frac{\alpha}{L^2}\right) f} \tag{26}$$

$$f = \frac{m\omega^2 L^2}{EA}, \quad \alpha = \frac{M_p}{mL} \tag{27}$$

where f is the non-dimensional frequency parameter and α is the mass ratio (attached mass/mass of CNT). m is the mass per unit length for nonlocal elasticity. The resultant shear force Π on the cross section of the nanotube is defined in the following equilibrium equation.

$$\Pi = \frac{\partial M}{\partial X} \tag{28}$$

N_t denotes the temperature dependent axial force with thermal expansion coefficient α. This constant force is defined as(S. Narendar (2010))

$$N_t = -EA\alpha T \tag{29}$$

where A is the cross section of nanotube and T is the temperature change. The longitudinal magnetic flux due to Lorentz force exerted on the tube in Z direction is represented by the term q_Z and is read from

$$q_Z = \eta A H_x^2 \frac{\partial^2 Y}{\partial X^2} - EA\alpha T \tag{30}$$

where H_x is the magnetic field strength and η is the magnetic permeability. For the Euler-beam theory the resultant bending moment M in Eq.(28) can be taken as follows

$$M = \int_A z\sigma_{xx} dA \tag{31}$$

where σ_{xx} is the nonlocal axial stress defined by nonlocal continuum theory. The constitutive Eq.(6) of a homogeneous isotropic elastic solid in nonlocal form for one-dimensional nanotube is taken as

$$\sigma_{xx} - (e_0 a)^2 \frac{\partial^2 \sigma_{xx}}{\partial X^2} = E\varepsilon_{xx} \tag{32}$$

where E is the Young's modulus of the tube, ε_{xx} is the axial strain, $(e_0 a)$ is a nonlocal parameter which represents the impact of nonlocal scale effect on the structure and a is the internal characteristic length. The nonlocal relations in Eq.(32) can be written with temperature environment as follows

$$\sigma_{xx} - (e_0 a)^2 \frac{\partial^2 \sigma_{xx}}{\partial X^2} = E\varepsilon_{xx} - E\alpha T. \tag{33}$$

In the context of Euler-Bernoulli beam model, the axial strain ε_{xx} for small deflection is defined as

$$\varepsilon_{xx} = -z\frac{\partial^2 Y}{\partial X^2} \tag{34}$$

where z is the transverse co-ordinate in the positive direction of deflection. By using Eqs. (33)-(34), in Eq.(31), the bending moment M can be expressed as

$$M - (e_0 a)^2 \left[\frac{\partial^2 M}{\partial X^2}\right] = EI^* \frac{\partial^2 Y}{\partial X^2} \tag{35}$$

$$\Pi - (e_0 a)^2 \left[\frac{\partial^2 M}{\partial X^2}\right] = F_{11}^S \frac{\partial Y}{\partial X} - C_{11}^S \frac{\partial^2 Y}{\partial X^2} \tag{36}$$

where $I = \int_A z^2 dA$ is the moment of inertia. By substituting Eq.(36) and (35) into Eq.(25), the nonlocal bending moment M and shear force Π can be expressed as follows

$$M - (e_0 a)^2 \left[(\rho A)\frac{\partial^2 Y}{\partial t^2} + q_{(mag)} - f(x) + EA\alpha T\right] = EI^* \frac{\partial^2 Y}{\partial X^2} \tag{37}$$

$$\Pi - (e_0 a)^2 \left[(\rho A)\frac{\partial^3 Y}{\partial X \partial t^2} + \frac{\partial^2 q_{(mag)}}{\partial X^2} - \frac{\partial f(x)}{\partial X} + EA\alpha T\right] = EI^* \frac{\partial^3 Y}{\partial X^3} + F_{11}^s \frac{\partial Y}{\partial X} - C_{11}^s \frac{\partial^2 Y}{\partial X^2}. \tag{38}$$

For the transverse vibration, the equation of motion (25) can be expressed that vibration of an elastic beam under distributed transverse pressure and thermal interaction with surrounding polymer elastic medium as

$$\begin{aligned} f(x) =& EI^* \frac{\partial^4 Y}{\partial X^4} + EA\alpha T \frac{\partial^2 Y}{\partial X^2} + (\rho A)\frac{\partial^2 Y}{\partial t^2} + \overline{q_z}(x) + F_s \frac{\partial^2 Y}{\partial X^2} \\ & - (e_0 a)^2 \left(EA\alpha T \frac{\partial^4 Y}{\partial X^4} + \overline{q_z}(x) + F_s \frac{\partial^4 Y}{\partial X^4} - \frac{\partial^2 f(x)}{\partial X^2} - \left(F_{11}^s \frac{\partial Y}{\partial X} - C_{11}^s \frac{\partial^2 Y}{\partial X^2}\right)\right) \end{aligned} \tag{39}$$

In addition, the pressure per unit axial length acting on the surface of the tube due to the surrounding elastic medium can be described by a Winkler-Pasternak type model(Barati (2017))

$$f(x) = -(-K_w + K_p + K_{nl}) \tag{40}$$

where K_w, K_p and K_{nl} are Winkler, Pasternak and nonlinear constant foundation. Substituting Eq.(40) into Eq.(39) yields

$$EI^* \frac{\partial^4 Y}{\partial X^4} + EA\alpha T \frac{\partial^2 Y}{\partial X^2} + \rho A \frac{\partial^2 Y}{\partial t^2} + \left(\eta A H_x^2 \frac{\partial^2 Y}{\partial X^2} + H_x \frac{\partial^2 Y}{\partial X^2}\right) \tag{41}$$

$$- (e_0 a)^2 \begin{pmatrix} EA\alpha T \frac{\partial^4 Y}{\partial X^4} + \rho A \frac{\partial^2 Y}{\partial X^2} + \left(\eta H_x^2 \frac{\partial^4 Y}{\partial X^4} - H_x \frac{\partial^4 Y}{\partial X^4}\right) \\ -(-K_w + K_p + K_{nl})\frac{\partial^2 Y}{\partial X^2} + \left(F_{11}^s \frac{\partial Y}{\partial X} - C_{11}^s \frac{\partial^2 Y}{\partial X^2}\right) \end{pmatrix} = -(-K_w + K_p + K_{nl}) \tag{42}$$

The surface piezoelectricity rigidities along the cross sectional area is modelled as

$$F_{11}^S = \left(\delta_{11}^S + \frac{e_{31} e_{31}^S}{k_{33}}\right)\frac{bh^2}{4} \tag{43}$$

$$C_{11}^S = \left(\delta_{11}^S + \frac{e_{31} e_{31}^S}{k_{33}}\frac{bh^2}{4}\right) \tag{44}$$

The flexoelectric nanotube is made PZT-5H where C_{11}^S is the elastic stiffness constant. The elastic properties are considered as C_{11} and the piezoelectric and dielectric coefficients are assumed as e_{31}, k_{33}(W. Yang (2015)). The flexoelectric coefficient as also considered as f_{31}]. The flexoelectric coefficient as also considered as f_{31} (W. Yang (2015)). The surface elastic and piezoelectric constants for PZT-5H can be considered as δ_{11}^S and e_{11}^S(Ebrahimi and Barati (2017a)).

4 Ultrasonic Wave Solution

Eq. (39) can be transformed in to frequency domain using Fourier transformation(S. Narendar (2010)):

$$Y(x,t) = \sum_{n=1}^{N} \hat{Y}(x) e^{-j(kn - \omega_n t)} \tag{45}$$

where $\hat{Y}$ is the amplitude of the wave motion, $j = \sqrt{-1}$, k is the wave number, ω_n the circular frequency of sampling point and N is the Nyquist frequency. The sampling rate and the number of sampling points should be sufficiently large to have relatively good resolution of both high and low frequencies respectively. Substitution of Eq.(45) into Eq.(40), we get

$$\sum_{n=1}^{N}\left[\left(EI^{*}\frac{\partial^4\hat{Y}}{\partial X^4}+EA\alpha T\frac{\partial^2\hat{Y}}{\partial X^2}+\rho A\frac{\partial^2\hat{Y}}{\partial t^2}+\left(\eta AH_x^2\frac{\partial^2\hat{Y}}{\partial X^2}+H_x\frac{\partial^2\hat{Y}}{\partial X^2}\right)\right.\right.$$
$$\left.\left.-(e_0a)^2\begin{pmatrix} EA\alpha T\frac{\partial^4\hat{Y}}{\partial X^4}+\rho A\frac{\partial^2\hat{Y}}{\partial X^2}+\left(\eta H_x^2\frac{\partial^4\hat{Y}}{\partial X^4}+H_x\frac{\partial^4\hat{Y}}{\partial X^4}\right) \\ -(-K_w+K_p+K_{nl})\frac{\partial^2\hat{Y}}{\partial X^2}+\left(F_{11}^{s}\frac{\partial\hat{Y}}{\partial X}-C_{11}^{s}\frac{\partial^2\hat{Y}}{\partial X^2}\right)+EA\alpha T\frac{\partial^2\hat{Y}}{\partial X^2}\end{pmatrix}\right)+(-K_w+K_p+K_{nl})\right]e^{i\omega_n t}=0 \tag{46}$$

This equation must be satisfied for each N and hence can be written as the ordinary differential equation in single variable X as,

$$\sum_{n=1}^{N}\left[\left(EI^{*}\frac{\partial^4\hat{Y}}{\partial X^4}+EA\alpha T\frac{\partial^4\hat{Y}}{\partial X^4}+\rho A\frac{\partial^2\hat{Y}}{\partial t^2}+\left(\eta AH_x^2\frac{\partial^2\hat{Y}}{\partial X^2}+H_x\frac{\partial^2\hat{Y}}{\partial X^2}\right)\right.\right.$$
$$\left.\left.-(e_0a)^2\begin{pmatrix} \rho A\frac{\partial^4\hat{Y}}{\partial X^2\partial t^2}-\left(\eta H_x^2\frac{\partial^2Y}{\partial X^2}+H_x\frac{\partial^2Y}{\partial X^2}\right) \\ -(-K_w+K_p+K_{nl})\frac{\partial^2\hat{Y}}{\partial X^2}-\left(F_{11}^{s}\frac{\partial\hat{Y}}{\partial X}-C_{11}^{s}\frac{\partial^2\hat{Y}}{\partial X^2}\right)\end{pmatrix}\right)+(-K_w+K_p+K_{nl})\right]e^{i\omega_n t}=0 \tag{47}$$

The above equation must be full filled for each values for small n and can be written in the following with single variable X. Eq.(46) can be reduced as

$$\left[\begin{array}{l} EI^{*}\frac{\partial^4\hat{Y}}{\partial X^4}+EA\alpha T\frac{\partial^4\hat{Y}}{\partial X^4}+\left(\eta AH_x^2\frac{\partial^2\hat{Y}}{\partial X^2}+H_x\frac{\partial^2\hat{Y}}{\partial X^2}\right)-\frac{\partial^2\rho A}{\partial t^2} \\ \left[\begin{array}{l}(\rho A-(-K_w+K_p+K_{nl})+EA\alpha T)\left(\eta AH_x^2\frac{\partial^2Y}{\partial X^2}-H_x\frac{\partial^2Y}{\partial X^2}\right)(e_0a)^2\frac{\partial^2\hat{Y}}{\partial X^2} \\ +\left(F_{11}^{s}\frac{\partial\hat{Y}}{\partial X}-C_{11}^{s}\frac{\partial^2\hat{Y}}{\partial X^2}\right)\end{array}\right]+(-K_w+K_p+K_{nl})\end{array}\right]=0 \tag{48}$$

The dimensionless variables are defined as

$$\begin{aligned} &\frac{X}{L}=x,\quad \frac{Y}{L}=y,\quad \alpha_i=\frac{I_i}{l},\quad \tau=\frac{e_0a}{l}, && K_w=\frac{k_wL^4}{EI^{*}D},\\ &F_{33}=F_{11}^{S}\frac{L^4}{EI^{*}C_{11}^{S}},\quad D=\frac{1}{12}C_{11}^{S}bh^3, && K_p=\frac{k_pL^4}{EI^{*}D}\\ &K_{nl}=\frac{k_{nl}L^4}{EI^{*}D},\quad \eta=\frac{1}{1+EA\alpha T},\quad \bar{N}_T=\frac{N_tL^2}{EI^{*}},\quad \delta_{11}^{S}=\frac{L^4}{EI^{*}} \end{aligned} \tag{49}$$

Substituting $\hat{Y}(x)=\hat{Y}e^{-i\omega x}$ into Eq.(49) employing Eq.(48) yields,

$$\left(1+EA\alpha T-\eta AH_x^2\right)\frac{\partial^4Y}{\partial x^4}+\left[EA\alpha T-\eta AH_x^2-(k_w+k_p+k_{nl})+\tau^2(F_{33})\right]\frac{\partial^2Y}{\partial x^2}$$
$$+2i\rho A\frac{\partial Y}{\partial x}-\left[\rho A+(k_w+k_p+k_{nl})\right]=0 \tag{50}$$

For non-trivial solution of the wave amplitude $\bar{Y}$ implies that,

$$\bar{Y}(x,t)=ye^{ik_nx} \tag{51}$$

Substituting Eq.(51) into Eq.(50), the following equation is obtained for non-trivial solution of the wave amplitude y

$$\left(1+EA\alpha T-\eta AH_x^2\right)k_n^4+\left[EA\alpha T-\eta aH_x^2-(-k_w+k_p+k_{nl})+\tau^2(F_{33})\right]k_n^2$$
$$+2i\rho Ak_n-\left[\rho A+(-k_w+k_p+k_{nl})\right]=0 \tag{52}$$

which represents the characteristic equation for a continuum structure (ECS) coupled with surrounding medium of an SWCNT.

5 Boundary Conditions

Here, an analytical solution of the governing equations for vibration of Nano beam having simply-supported (S-S) and clamped-clamped (C-C) boundary condition is presented which are given as below:

5.1 Simply supported SWCNT

The boundary conditions for the simply supported problem are $(X) = (0, L)$,

$$
\begin{aligned}
&Y(X)\,|_{X=0} = 0,\\
&M(X) = \left(-EI^{*}\frac{\partial^2 Y(X)}{\partial X^2} + (e_0a)^2\left[(\rho A)\frac{\partial^2 Y(X)}{\partial t^2} + q_{(mag)}\frac{\partial^2 Y(X)}{\partial X^2} - f(x)\frac{\partial^2 Y(X)}{\partial X^2} + EA\alpha T\frac{\partial^2 Y(X)}{\partial X^2}\right]\right)_{X=0} = 0,\\
&Y(X)\,|_{X=L} = 0\\
&M(X) = \left(-EI^{*}\frac{\partial^2 Y(X)}{\partial X^2} + (e_0a)^2\left[(\rho A)\frac{\partial^2 Y(X)}{\partial t^2} + q_{(mag)}\frac{\partial^2 Y(X)}{\partial X^2} - f(x)\frac{\partial^2 Y(X)}{\partial X^2} + EA\alpha T\frac{\partial^2 Y(X)}{\partial X^2}\right]\right)_{X=L} = 0,\\
&Y(X)\,|_{X=0} = 0,\\
&\Pi(X) = \left(-\left(EI^{*}\frac{\partial^3 Y(X)}{\partial X^3} + F_{11}^{S}\frac{\partial Y(X)}{\partial X} - C_{11}^{S}\frac{\partial^2 Y(X)}{\partial X^2}\right) + (e_0a)^2\left[(\rho A)\frac{\partial^3 Y(X)}{\partial X^2\partial t} + \frac{\partial^2 q_{(mag)}}{\partial X^2} - \frac{\partial f(x)}{\partial X} + EA\alpha T\right]\right)_{X=0} = 0,\\
&Y(X)\,|_{X=L} = 0,\\
&\Pi(X) = \left(-\left(EI^{*}\frac{\partial^3 Y(X)}{\partial X^3} + F_{11}^{S}\frac{\partial Y(X)}{\partial X} - C_{11}^{S}\frac{\partial^2 Y(X)}{\partial X^2}\right) + (e_0a)^2\left[(\rho A)\frac{\partial^3 Y(X)}{\partial X^2\partial t} + \frac{\partial^2 q_{(mag)}}{\partial X^2} - \frac{\partial f(x)}{\partial X} + EA\alpha T\right]\right)_{X=L} = 0,
\end{aligned}
\tag{53}
$$

5.2 Clamped - Clamped SWCNT

Assume the case where both the ends of the beam are clamped and are subjected to axial compressive load. The boundary conditions for this case are given as

$$
\begin{aligned}
&Y(X)\,|_{X=0} = 0, \quad \left.\frac{\partial Y(X)}{\partial X^2}\right|_{X=0} = 0,\\
&Y(X)\,|_{X=L} = 0, \quad \left.\frac{\partial Y(X)}{\partial X^2}\right|_{X=L} = 0.
\end{aligned}
\tag{54}
$$

6 Numerical Results and Discussion

In this section, the armchair SWCNT embedded in a polymer matrix subjected to magneto-thermo elastic forces is considered as an example for the nonlinear vibration analysis. The geometrical and material parameters taken for the numerical verification is shown in Table 1. Table 2 present the comparative study between the numerical results of maximum transverse deflection of C-C CNT with and without surface effects. Results predict the reasonable agreement with the literature.

Tab. 1: Material properties H. Lee (2009), P. Lata (2019a) and Ebrahimi and Barati (2017a)

Materials	PZT
EI	$1.1122 \times 10^{-25}\mathrm{Nm}^9$
α^0	$-1.5 \times 10^{-6}\mathrm{C}^{-1}$
ρ	$2.3\mathrm{g/cm}^3$
e_0	0.31nm
a	0.142N/m
E_s	35.3N/m
μ	$4\pi \times 10^{-7}$N/m
H_x	2×10^{8}A/m
f_{31}	10^{-7}C/(Vm)
c_{11}	102Gpa
δ_{11}^{S}	102N/m
e_{31}^{S}	-3×10^{-8}C/m
k_{33}	1.76×10^{-8}C/(Vm)

Tab. 2: Comparison of maximum transverse deflection in C-C nanotube incorporating surface effects(S.E) R. Basutkar (2019)

	BASUTKAR, et al.		**Author**	
(L/h)	$(S.E = 0)$	$(S.E \neq 0)$	$(S.E = 0)$	$(S.E \neq 0)$
10	0.6343	0.6334	0.6396	0.6363
15	0.9472	0.9459	0.9450	0.9432
20	1.2550	1.2530	1.2934	1.2914

Figs.4 and 5 investigated the effect of dimensionless frequency versus non dimensional amplitude for various nonlocal parameters through $L/h = 10$ and $L/h = 20$, $V = 0$, $K_p = 20$, $\Delta T = 20$ and $\alpha = 0.5$ respectively and it is found that increasing value of amplitude caused increase of dimensionless frequency. When nonlocal parameter arises the magnitude of frequency decreases, and we understand from this subject that nonlocal values has significant role under frequency. But a softening behaviour is observed in frequency due to the rise in slenderness in Fig.5.

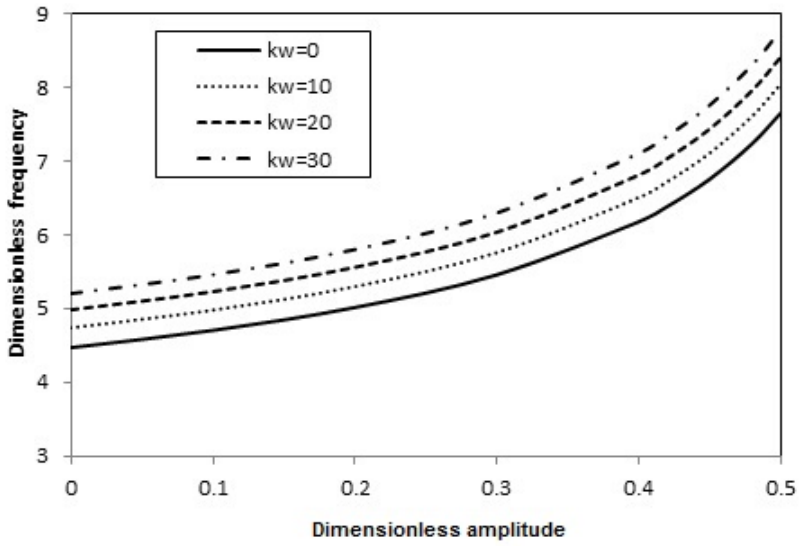

Fig. 4: Graph of dimensionless frequency versus dimensionless amplitude for various Pasternak foundation values($L/h = 10$, $V = 5$, $K_p = 20$, $\Delta T = 20$, $\alpha = 0.5$)

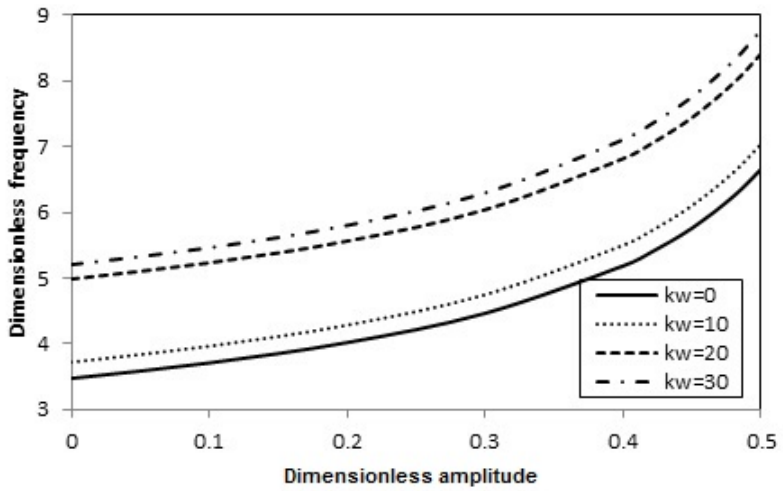

Fig. 5: Graph of dimensionless frequency versus dimensionless amplitude for various Pasternak foundation values ($L/h = 10$, $V = 5$, $K_p = 20$, $\Delta T = 30$, $\alpha = 0.5$)

Variation of dimensionless frequency of nanotube with respect to non-dimensional amplitude via various voltage values with $L/h = 10 - 20$, $\alpha = 0.5$, $K_p = K_w = 20 - 30$ and $\Delta T = 20$, are presented in Figs.6 and 7. It is found, rise in non-dimensional amplitude caused that increasing of dimensionless frequency of nanotube through various voltage values. So the axial tensile and compressive forces produced in the nanotubes via the constructed positive and negative voltages, respectively. In addition, it is lightly observed that the dimensionless frequency is lightly dependent on slenderness ratio and foundation parameter for constant

temperature value ($\Delta T = 20$).

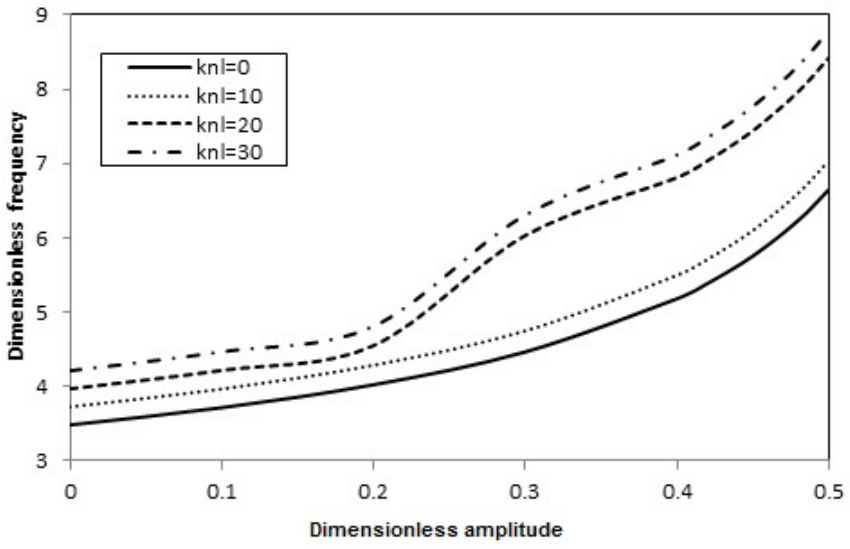

Fig. 6: Graph of dimensionless frequency versus dimensionless amplitude for various nonlinear foundation values ($L/h = 10$, $V = 0$, $K_w = K_p = 10$, $\Delta T = 10$, $\alpha = 0.5$)

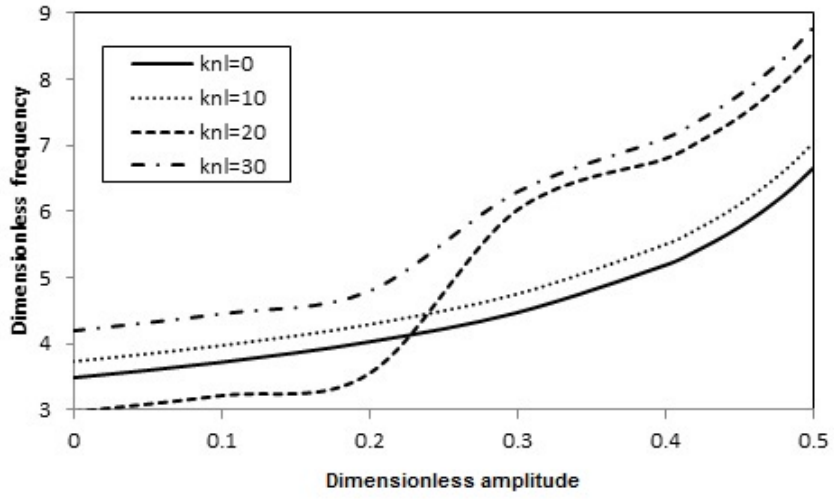

Fig. 7: Graph of dimensionless frequency versus dimensionless amplitude for various nonlinear foundation values ($L/h = 20$, $V = 0$, $K_w = K_p = 20$, $\Delta T = 20$, $\alpha = 0.5$)

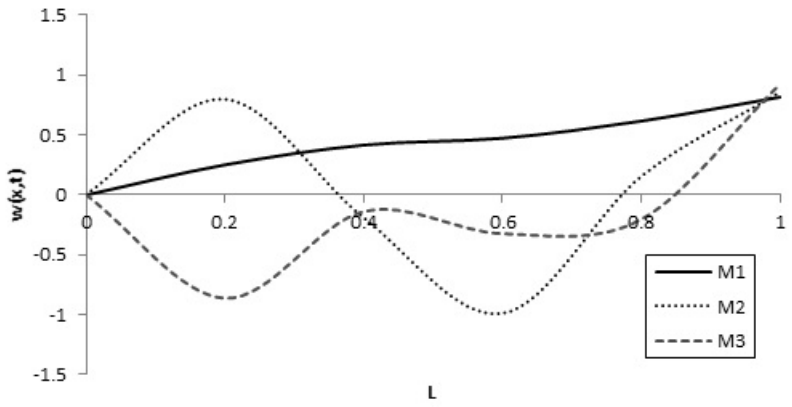

Fig. 8: Graph of bending moment versus length for various modes ($L/h = 10$, $V = 0$, $K_w = K_p = 20$, $\Delta T = 20$, $\Delta H = 10$, $\alpha = 0.5$)

Figs.8 and 9 demonstrates the variation of bending moment along the first three modes versus length of the nanotube for $L/h = 10$,

$V = 0$, $\alpha = 0.5$, $K_w = K_p = 20$, $\Delta T = 20$, $\Delta H = 10$. It is referred from these figures that as the length grows the bending moment is attaining tensile and compressive nature while growing through higher modes. Also, the influence of magnetic field effect is observed in the wave trend.

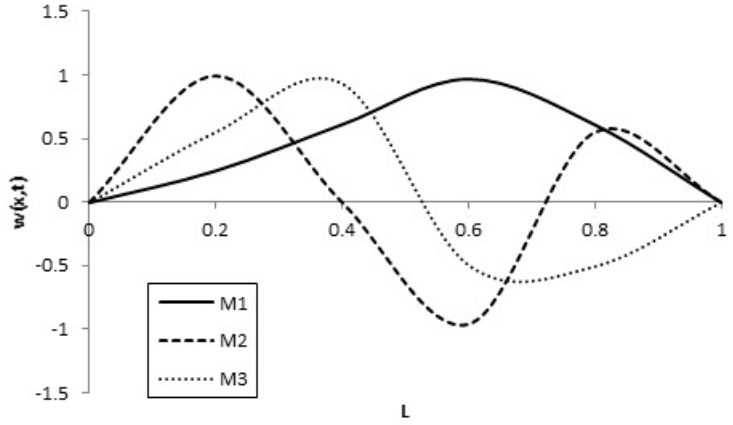

Fig. 9: Graph of bending moment versus length for various modes ($L/h = 10$, $V = 0$, $K_w = K_p = 20$, $\Delta T = 20$, $\Delta H = 20$, $\alpha = 0.5$)

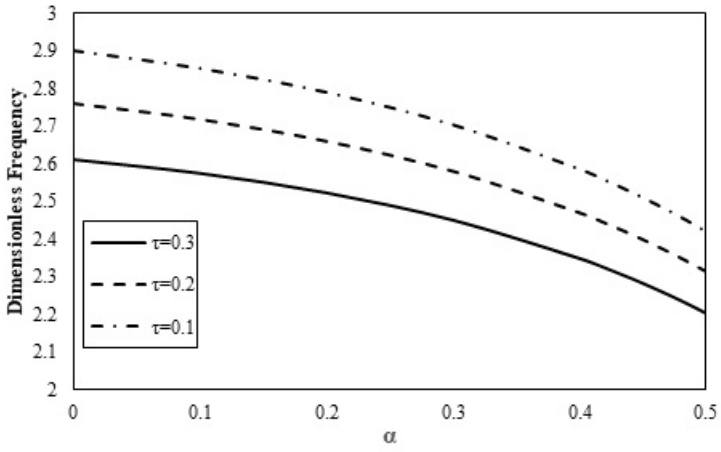

Fig. 10: Graph of dimensionless frequency versus attached mass ratio($L/h = 10$, $V = 0.2$, $K_w = K_p = 20$, $\Delta T = 10$, $\Delta H = 10$)

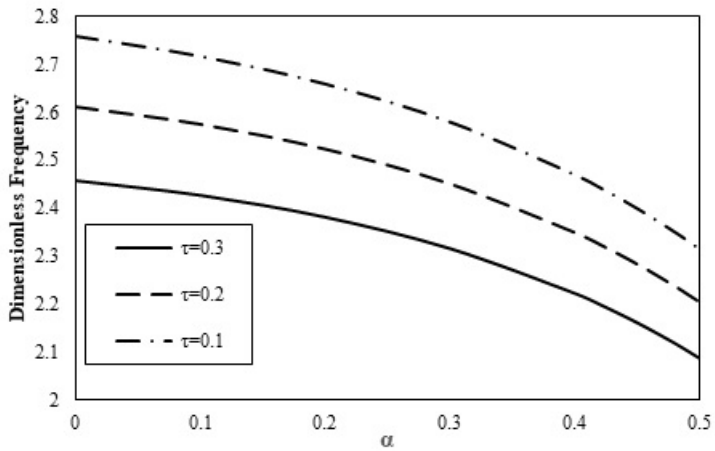

Fig. 11: Graph of dimensionless frequency versus attached mass ratio($L/h = 10$, $V = 0.2$, $K_w = K_p = 20$, $\Delta T = 20$, $\Delta H = 20$)

Figs.10 and 11 presents the variation of dimensionless frequency versus attached mass ratio through $L/h = 10$, $V = 0.2$, $K_w = K_p = 20$ for different environmental conditions $(\Delta T, \Delta C) = (10, 10), (20, 20)$. It is seen that the frequency parameter decreases as the attached mass ratio values increases. It should be pointed out that thermal and hygro-thermal environment degrades the plate stiffness via increasing attached mass ratio. It is found that effects of temperature and moisture concentration

rise are more prominent at lower values of mass ratio. Generally, by attaching a particle to the dynamics of SWCNT, the total mass of the system amplifies but stiffness remains unchanged and as a result frequency decreases. The effect of nonlocality can also be seen from the figure. Increasing the nonlocal parameter decreases the frequency parameter.

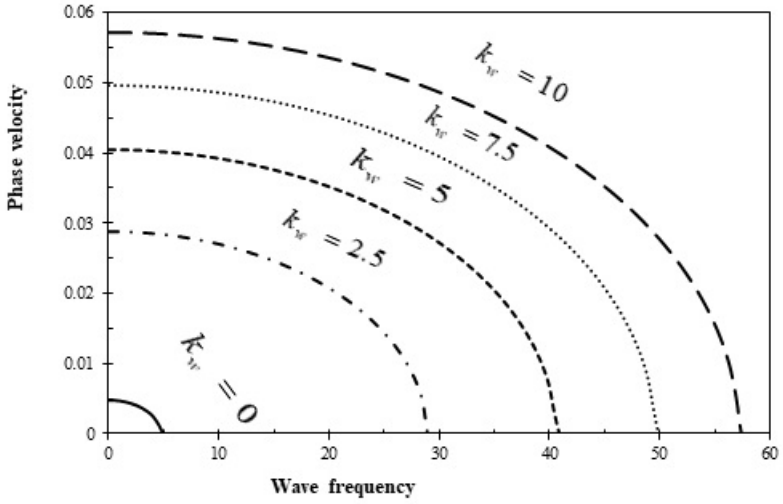

Fig. 12: Variation of phase velocity versus wave frequency for different Winkler coefficients

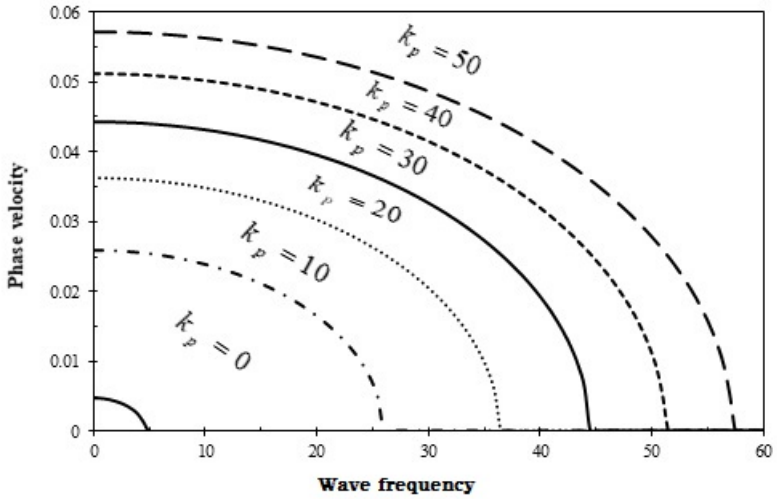

Fig. 13: Variation of phase velocity versus wave frequency for different Pasternak coefficients

Now, the effect of Winkler and Pasternak coefficients are going to be investigated by plotting the wave frequency versus phase velocity in Figs.12 and 13. It is clearly visible that both of the Winkler (linear) and Pasternak (nonlinear) coefficients have enough potential to amplify wave frequency values. Moreover, it is significant to point that the most mentionable change in the wave frequency responses can be observed once Winkler coefficient is changed from $k_w = 0$ to $k_w = 2.5$. To make it simply understandable, the first change in the Winkler or Pasternak coefficient's value from zero to the first nonzero value has the highest efficiency in making wave frequency bigger.
The variations of the flexoelectricity versus the wave number via various Pasternak and Winkler parameters are shown in Figs.14 and 15, respectively. It is found from this figure that regardless of the magnitude of foundation parameter, the flexoelectricity amplifies its magnitude in higher values of wave number, from this it is referred that the stiffness of the nanotube is hardening through this type of coupling effect. It must be mentioned that at a variable foundation parameters, the increase of flexoelectricity with wave number has been experienced oscillating behaviour in energy transfer.

7 Conclusion

This paper presents the study of nonlinear magneto-flexo-thermo elastic waves in an armchair SWCNT resting on polymer matrix via Euler beam theory. The analytical formulation is developed based on Eringen's nonlocal elasticity theory to account small scale effect. This medium is embedded in a nonlinear foundation supported by Winkler-Pasternak model. The solution is obtained by ultrasonic wave dispersion relations. Parametric work is introduced to scrutinize the influence of the magneto-electro-mechanical loadings, nonlocal parameter, and aspect ratio on the deflection characteristics of nanotube. The findings are summarized as

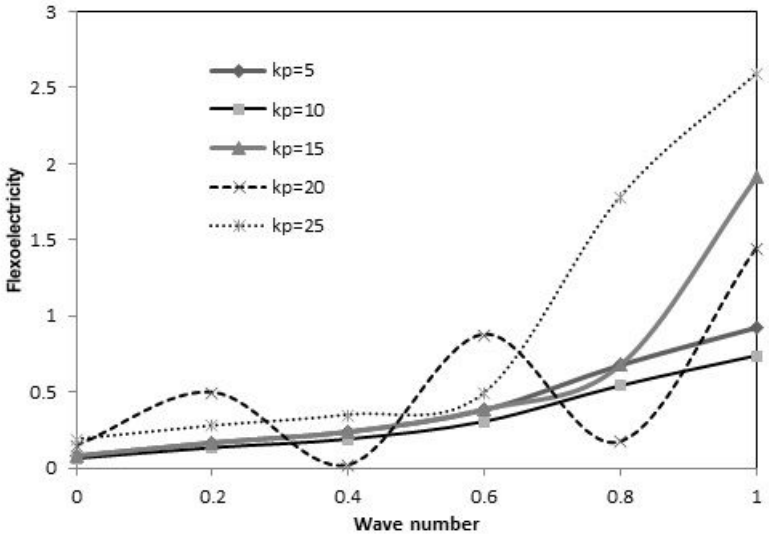

Fig. 14: Variation of flexoelectricity versus wave number for different Pasternak coefficients

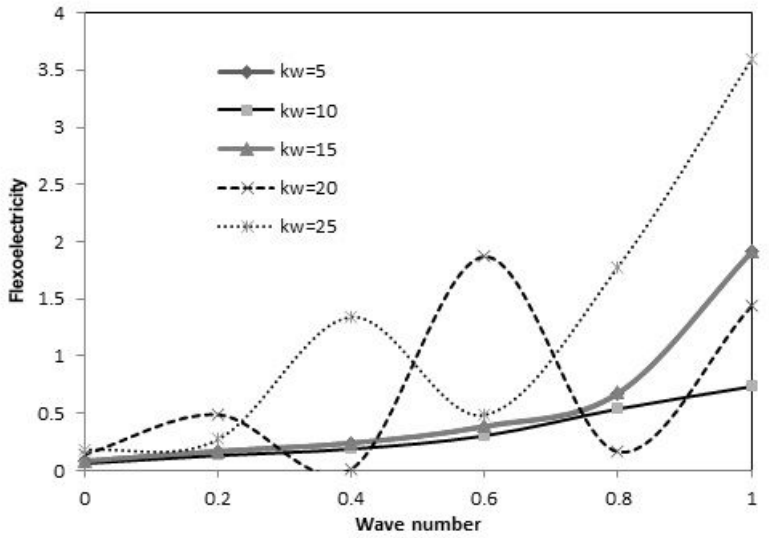

Fig. 15: Variation of flexoelectricity versus wave number for different Winkler coefficients

- It is observed that the increase in the foundation constants raises the stiffness of the medium.
- The result also shows that as the dimensionless amplitude enhances the non-dimensional frequency via nonlinear foundation parameter.
- It was observed that embedding the structure on an elastic foundation is able to improve the dynamic behavior of the armchair nanotube. Moreover, it was understood that the Pasternak parameter can affect the structure more than the Winkler parameter.
- It is found that the vibration modes of SWCNT are softened with attached mass and small length scale values.
- Present assessment reveals that adding Winkler or Pasternak parameter may be answered by a reduction in the magnitude of phase velocity.
- Also, numerical investigations predict amplification in flexoelectricity via raise in wave number values once foundation parameter is enhanced.

References

A. Besseghier H. Heireche N. Moulay L. Boumia A. Benzair, A. Tounsi. The thermal effect on vibration of single-walled carbon nanotubes using nonlocal timoshenko beam theory. *Journal of Physics D: Applied Physics*, 41(22):225404(1–10), 2008. doi: 10.1088/0022-3727/41/22/225404.

M. S. Houari A. Benzair L. Boumia H. Heireche A. Besseghier, A. Tounsi. Thermal effect on wave propagation in double-

walled carbon nanotubes embedded in a polymer matrix using nonlocal elasticity. *Physica E: Low-dimensional Systems and Nanostructures*, 43(7):1379–1386, 2011. doi: 10.1016/j.physe.2011.03.008.

D. G. B. Edelen A. C. Eringen. On nonlocal elasticity. *International journal of engineering science*, 10(3):233–248, 1972. doi: 10.1016/0020-7225(72)90039-0.

S. Amir A. G. Arani, M. Roudbari. Longitudinal magnetic field effect on wave propagation of fluid-conveyed swcnt using knudsen number and surface considerations. *Applied Mathematical Modelling*, 40(3):2025–2038, 2016. doi: 10.1016/j.apm.2015.09.055.

S. Mahmoud H. Heireche A. Tounsi A. Semmah, O. A. Beg. Thermal buckling properties of zigzag single-walled carbon nanotubes using a refined nonlocal model. *Advances in Materials Research*, 3(2):77–89, 2014. doi: 10.12989/amr.2014.3.2.077.

M. Aydogdu. Axial vibration analysis of nanorods (carbon nanotubes) embedded in an elastic medium using nonlocal elasticity. *Mechanics Research Communications*, 43:34–40, 2012. doi: 10.1016/j.mechrescom.2012.02.001.

H. R. Azarboni. Magneto-thermal primary frequency response analysis of carbon nanotube considering surface effect under different boundary conditions. *Composites Part B: Engineering*, 165:435–441, 2019. doi: 10.1016/j.compositesb.2019.01.093.

C. P. Zhang Y. Tang B. Fang, Y. X. Zhen. Nonlinear vibration analysis of double-walled carbon nanotubes based on nonlocal elasticity theory. *Applied Mathematical Modelling*, 37(3):1098–1107, 2013. doi: 10.1016/j. aprm.2012.03.032.

S. M. Hasheminejad B. Gheshlaghi. Surface effects on nonlinear free vibration of nanobeams. *Composites Part B: Engineering*, 42(4):934–937, 2011. doi: 10.1016/j.compositesb.2010.12.026.

M. R. Barati. Investigating nonlinear vibration of closed circuit flexoelectric nanobeams with surface effects via hamiltonian method. *Microsystem Technologies*, 24(4):1841–1851, 2017. doi: 10.1007/s00542-017-3549-8.

C. S. Chen H. H. Chen D. H. Wu, W. T. Chien. Resonant frequency analysis of fixed-free single-walled carbon nanotube-based mass sensor. *Sensors and Actuators A: Physical*, 126(1):117–121, 2006. doi: 10.1016/j.sna.2005.10.005.

Z. Shen D. Zhang, Y. Lei. Vibration analysis of horn-shaped single-walled carbon nanotubes embedded in viscoelastic medium under a longitudinal magnetic field. *International Journal of Mechanical Sciences*, 118:219–230, 2016. doi: 10.1016/j.ijmecsci.2016.09.025.

F. Ebrahimi and M. R. Barati. Surface effects on the vibration behavior of flexoelectric nanobeams based on nonlocal elasticity theory. *The European Physical Journal Plus*, 132(1), 2017a. doi: 10.1140/epjp/i2017-11320-5.

F. Ebrahimi and M. R. Barati. Vibration analysis of piezoelectrically actuated curved nanosize fg beams via a nonlocal strain-electric field gradient theory. *Mechanics of Advanced Materials and Structures*, 25(4):350–359, 2017b. doi: 10.1080/15376494.2016.1255830.

F. Ebrahimi and A. Dabbagh. Magnetic field effects on thermally affected propagation of acoustical waves in rotary double-nanobeam systems. *Waves in Rando Complex Media*, pages 1–21, 2018. doi: 10.1080/17455030.2018.1558308.

A. C. Eringen. On differential equations of nonlocal elasticity and solutions of screw dislocation and surface waves. *Journal of Applied Physics*, 54(9):4703–4710, 1983. doi: 10.1063/1.332803.

A. C. Eringen. *Nonlocal continuum field theories*. Springer, Berlin, 2002.

O. Civalek M. Vinyas F. Ebrahimi, M. Mahsa Karimisal. Surface effect on scale -dependent vibration behaviour of flexoelectric sandwhich nanobeams. *Advances in Nano Research*, 70(2):77–88, 2019. doi: 10.12989/anr.2019.7.2.077.

U. Güven. General investigation for longitudinal wave propagation under magnetic field effect via nonlocal elasticity. *Applied Mathematics and Mechanics*, 36(10):1305–1318, 2015. doi: 10.1007/s10483-015-1985-9.

E. Esmailzadeh H. Askari. Forced vibration of fluid conveying carbon nanotubes considering thermal effect and nonlinear foundations. *Composites Part B: Engineering*, 113:31–43, 2017. doi: 10.1016/j.compositesb.2016.12.046.

M. Zidour A. Benzair H. Baghdadi, A. Tounsi. Thermal effect on vibration characteristics of armchair and zigzag single-walled carbon nanotubes using nonlocal parabolic beam theory. *Fullerenes, Nanotubes and Carbon Nanostructures*, 23(3):266–272, 2014. doi: 10.1080/1536383x.2013.787605.

A. Abdelkefi Y. Hong L. Wang H. Dai, S. Ceballes. Exact modes for post-buckling characteristics of nonlocal nanobeams in a longitudinal magnetic field. *Applied Mathematical Modelling*, 55:758–775, 2018. doi: 10.1016/j.apm.2017.11.025.

A. Benzair M. Maachou E. A. Bedia H. Heireche, A. Tounsi. Sound wave propagation in single-walled carbon nanotubes using nonlocal elasticity. *Physica E: Low-dimensional Systems and Nanostructures*, 40(8):2791–2799, 2008. doi: 10.1016/j.physe.2007.12.021.

W. Chang H. Lee. Vibration analysis of a viscous-fluid-conveying single-walled carbon nanotube embedded in an elastic medium. *Physica E: Low-dimensional Systems and Nanostructures*, 41(4):529–532, 2009. doi: 10.1016/j.physe.2008.10.002.

W. Chang H. Lee, J. Hsu. Frequency shift of carbon-nanotube-based mass sensor using nonlocal elasticity theory. *Nanoscale Research Letters*, 5(11):1774–1778, 2010. doi: 10.1007/s11671-010-9709-8.

Z. Lyu H. Liu. Modeling of novel nanoscale mass sensor made of smart fg magneto-electro-elastic nanofilm integrated with graphene layers. *Thin-Walled Structures*, 151:106749, 2020. doi: 10.1016/j.tws.2020.106749.

W. J. Chang J. C. Hsu, R P. Chang. Resonance frequency of chiral single walled carbon nanotubes using timoshenko beam theory. *Physics Letters A*, 373(8):2757–2759, 2008. doi: 10.1016/j.physleta.2008.01.007.

S. Zeng K. Wang, B. Wang. Analysis of an array of flexoelectric layered nanobeams for vibration energy harvesting. *Composite Structures*, 187:48–57, 2018. doi: 10.1016/j.compstruct.2017.12.040.

L. Ling L. Li, Y. Hu. Wave propagation in viscoelastic single-walled carbon nanotubes with surface effect under magnetic field based on nonlocal strain gradient theory. *Physica E: Low-dimensional Systems and Nanostructures*, 75:118–124, 2016. doi: 10.1016/j.physe.2015.09.028.

W. Guo L. Wang, H. Hu. Validation of the non-local elastic shell model for studying longitudinal waves in single-walled carbon nanotubes. *Nanotechnology*, 17:1408–1415, 2006. doi: 10.1088/0957-4484/17/5/041.

M. Hosseini M. A. Nematollahi, B. Jamali. Fluid velocity and mass ratio identification of piezoelectric nanotube conveying fluid using inverse analysis. *Acta Mechanica*, 231(2):683–700, 2019. doi: 10.1007/s00707-019-02554-0.

M. Aydogdu M. Arda. Vibration analysis of carbon nanotube mass sensors considering both inertia and stiffness of the detected mass. *Mechanics Based Design of Structures and Machines*, pages 1–17, 2020. doi: 10.1080/15397734.2020.1728548.

S. Filiz M. Aydogdu. Modeling carbon nanotube-based mass sensors using axial vibration and nonlocal elasticity. *Physica E: Low-dimensional Systems and Nanostructures*, 43(6):1229–1234, 2011. doi: 10.1016/j.physe.2011.02.006.

A. Semmah M. S. Houari A. Benzair A. Tounsi M. Naceri, M. Zidour. Sound wave propagation in armchair single walled carbon nanotubes under thermal environment. *Journal of Applied Physics*, 110(12):124322, 2011. doi: 10.1063/1.3671636.

H. Shahverdi M. R. Barati. Frequency analysis of nanoporous mass sensors based on a vibrating heterogeneous nanoplate and nonlocal strain gradient theory. *Microsystem Technologies*, 24(3):1479–1494, 2017. doi: 10.1007/s00542-017-3531-5.

H. Kwon M. Sadeghi-Goughari, S. Jeon. Effects of magnetic-fluid flow on structural instability of a carbon nanotube conveying nanoflow under a longitudinal magnetic field. *Physics Letters A*, 381(35):2898–2905, 2017. doi: 10.1016/j.physleta.2017.06.054.

K. H. Benrahou A. Tounsi E. A. Bedia L. Hadji M. Zidour, T. H. Daouadji. Buckling analysis of chiral single-walled carbon nanotubes by using the nonlocal timoshenko beam theory. *Mechanics of Composite Materials*, 50(1):95–104, 2014. doi: 10.1007/s11029-014-9396-0.

I. Kaur P. Lata. Thermomechanical interactions due to time harmonic sources in a transversely isotropic magneto thermoelastic solids with rotation. *International Journal of Microstructure and Materials Properties*, 14(6):549, 2019a. doi: 10.1504/ijmmp.2019.103190.

I. Kaur P. Lata. Transversely isotropic thick plate with two temperature and gn type-iii in frequency domain. *Coupled System Mechanics*, 8(1):55–70, 2019b. doi: 10.12989/csm.2019.8.1.055.

N. Sharma P. Lata, R. Kumar. Plane waves in anisotropic thermo-elastic medium. *Steel and Composite Structures*, 22(3):567–587, 2016. doi: 10.12989/scs.2016.22.3.567.

S. Quek Q. Wang, V. Varadan. Small scale effect on elastic buckling of carbon nanotubes with nonlocal continuum models. *Physics Letters A*, 357(2):130–135, 2006. doi: 10.1016/j.physleta.2006.04.026.

S. Sahmani R. Ansari, R. Gholami. On the dynamic stability of embedded single-walled carbon nanotubes including thermal environment effects. *Scientia Iranica*, 19(3):919–925, 2012. doi: 10.1016/j.scient.2012.02.013.

M. Ray R. Basutkar, S. Sidhardh. Static analysis of flexoelectric nanobeams incorporating surface effects using element free galerkin method. *European Journal of Mechanics - A/Solids*, 76:13–24, 2019. doi: 10.1016/j.euromechsol.2019.02.013.

J. Mitchell R. Chowdhury, S. Adhikari. Vibrating carbon nanotube based bio-sensors. *Physica E: Low-dimensional Systems and Nanostructures*, 42(2):104–109, 2009. doi: 10.1016/j.physe.2009.09.007.

P. Lata S. M. Abo-Dahab R. Kumar, N. Sharma. Rayleigh waves in anisotropic magneto thermo-elastic medium. *Coupled System Mechanics*, 6(3):317–333, 2017. doi: 10.12989/csm.2017.6.3.317.

F. Ebrahimi R. Selvamani, M. Mahaveer Sree Jayan. Static stability analysis of mass sensors consisting of hygro-thermally activated graphene sheets using a nonlocal strain gradient theory. *Engineering transactions*, 68(3):269–295, 2020. doi: 10.24423/engtrans.1187.20200904.

O. D. Makinde R. Selvamani. Influence of rotation on transversely isotropic piezoelectric rod coated with a thin film. *Engineering transactions*, 66(3):211–227, 2018. doi: 10.24423/engtrans.859.20180726.

S. Gopalakrishnan S. Narendar. Ultrasonic wave characteristics of nanorods via nonlocal strain gradient models. *Journal of Applied Physics*, 107(8):084312, 2010. doi: 10.1063/1.3345869.

S. Gopalakrishnan S. Narendar, D. R. Mahapatra. Prediction of nonlocal scaling parameter for armchair and zigzag single-walled carbon nanotubes based on molecular structural mechanics, nonlocal elasticity and wave propagation. *International Journal of Engineering Science*, 49(6):509–522, 2011. doi: 10.1016/j.ijengsci.2011.01.002.

J. Phadikar S. Pradhan. Small scale effect on vibration of embedded multilayered graphene sheets based on nonlocal continuum models. *Physics Letters A*, 373(11):1062–1069, 2009. doi: 10.1016/j.physleta.2009.01.030.

M. Zidour A. Tounsi-E. A. Bedia T. Bensattalah, T. H. Daouadji. Investigation of thermal and chirality effects on vibration of single-walled carbon nanotubes embedded in a polymeric matrix using nonlocal elasticity theories. *Mechanics of Composite Materials*, 52(4):555–568, 2016. doi: 10.1007/s11029-016-9606-z.

A. Semmah A. Tounsi-S. R. Mahmoud W. A. Bedia, A. Benzair. On the thermal buckling characteristics of armchair single-walled carbon nanotube embedded in an elastic medium based on nonlocal continuum elasticity. *Brazilian Journal of Physics*, 45(2):225–233, 2015. doi: 10.1007/s13538-015-0306-2.

S. Shen W. Yang, X. Liang. Electromechanical responses of piezoelectric nanoplates with flexoelectricity. *Acta Mechanica*, 226 (9):3097–3110, 2015. doi: 10.1007/s00707-015-1373-8.

Q. Wang. Wave propagation in carbon nanotubes via nonlocal continuum mechanics. *Journal of Applied Physics*, 98(12):124301–6, 2005. doi: https://doi:org/10.1063/1.2141648.

J. Shi Q. Ni X. Lei, T. Natsuki. Surface effects on the vibrational frequency of double-walled carbon nanotubes using the nonlocal timoshenko beam model. *Composites Part B: Engineering*, 43(1):64–69, 2012. doi: 10.1016/j.compositesb.2011.04.032.

G. R. Liu Y. Q. Zhang, X. Liu. Thermal effect on transverse vibrations of double-walled carbon nanotubes. *Nanotechnology*, 18 (44):445701(1–7), 2007. doi: 10.1088/0957-4484/18/44/445701.

A. Leung W. Zhong Y. Wu, X. Zhang. An energy-equivalent model on studying the mechanical properties of single-walled carbon nanotubes. *Thin-Walled Structures*, 44(6):667–676, 2006. doi: 10.1016/j.tws.2006.05.003.

Y. Tang Y. Zhen, S. Wen. Free vibration analysis of viscoelastic nanotubes under longitudinal magnetic field based on nonlocal strain gradient timoshenko beam model. *Physica E: Low-dimensional Systems and Nanostructures*, 105:116–124, 2019. doi: 10.1016/j.physe.2018.09.005.

T. Yamabe. Recent development of carbon nanotube. *Synthetic Metals*, 70(1-3):1511–1518, 1995. doi: 10.1016/0379-6779(94)02939-v.

E. Esmailzadeh Z. Saadatnia. Nonlinear harmonic vibration analysis of fluid-conveying piezoelectric-layered nanotubes. *Composites Part B: Engineering*, 123:193–209, 2017. doi: 10.1016/j.compositesb.2017.05.012.

L. Y. Jiang Z. Yan. The vibrational and buckling behaviors of piezoelectric nanobeams with surface effects. *Nanotechnology*, 22 (24):245703, 2011. doi: 10.1088/0957-4484/22/24/245703.